

¹ The Evolution of Siphonophore Tentilla as Specialized Tools for Prey Capture

³ Alejandro Damian-Serrano^{1,‡}, Steven H.D. Haddock², Casey W. Dunn¹

⁴ ¹ Yale University, Department of Ecology and Evolutionary Biology, 165 Prospect St.,
⁵ New Haven, CT 06520, USA

⁶ ² Monterey Bay Aquarium Research Institute, 7700 Sandholdt Rd., Moss Landing, CA
⁷ 95039, USA

⁸ [‡] Corresponding author: Alejandro Damian-Serrano, email: alejandro.damianserrano@
⁹ yale.edu

¹⁰ Abstract

¹¹ Predators have evolved dedicated body parts to capture and subdue prey. As different
¹² predators specialize on distinct prey taxa, their tools for prey capture diverge into a variety
¹³ of adaptive forms. Studying the evolution of predation is facilitated by a predator clade with
¹⁴ structures used exclusively for prey capture and with significant morphological variation.
¹⁵ Siphonophores, a clade of colonial cnidarians, satisfy these criteria particularly well, cap-
¹⁶ turing prey with their tentilla (tentacle side branches). Earlier work has shown that extant
¹⁷ siphonophore diets correlate with the different morphologies and sizes of their tentilla and
¹⁸ nematocysts. We hypothesize that evolutionary specialization on different prey types has
¹⁹ driven the phenotypic evolution of these characters. To test this hypothesis, we: (1) mea-
²⁰ sured multiple morphological traits from fixed siphonophore specimens using microscopy and
²¹ high-speed video techniques, (2) mapped these data to a phylogenetic tree of 45 species, and
²² (3) analyzed the evolutionary associations between siphonophore nematocyst characters and
²³ prey type data from the literature. Our results show that siphonophore tentillum structure
²⁴ has strong evolutionary associations with prey type and size specialization, and suggest that
²⁵ shifts between prey-type specializations are linked to shifts in tentillum and nematocyst

²⁶ size and shape. We found that predatory specialists can evolve into generalists, and that
²⁷ specialists on one prey type have directly evolved into specialists on other prey types. Thus,
²⁸ the evolutionary history of tentilla shows that siphonophores are an example of ecological
²⁹ niche diversification via morphological innovation and evolution. This study contributes to
³⁰ understanding how morphological evolution has shaped present-day oceanic food webs.

³¹ **Keywords**

³² Siphonophores, tentilla, nematocysts, predation, specialization, character evolution

³³

³⁴ Most animal predators have characteristic biological tools that they use to capture and
³⁵ subdue prey. Raptors have claws and beaks, snakes have fangs, wasps have stingers, and
³⁶ cnidarians have nematocyst-laden tentacles. The functional morphology of these structures
³⁷ tend to be finely attuned to their ability to successfully capture specific prey (Schmitz
³⁸ 2017). Long-term adaptive evolution in response to the defense mechanisms of the prey (*e.g.*
³⁹ avoidance, escape, protective barriers) leads to modifications that can counter those defenses
⁴⁰ The more specialized the diet of a predator is, the more specialized its tools need to be to
⁴¹ meet the specific challenges posed by the prey. Understanding the relationships between
⁴² predatory specializations and morphological specializations is necessary to contextualize the
⁴³ phenotypic diversity of predators, and to quantify the importance of ecological diversification
⁴⁴ in generating this diversity.

⁴⁵ Siphonophores (Cnidaria : Hydrozoa) are a clade of organisms bearing modular structures
⁴⁶ that are exclusively used for prey capture: the tentilla (Fig. 1). These present a significant
⁴⁷ morphological variation across species (Mapstone 2014) (Fig. 2), which makes them an
⁴⁸ ideal system to study the relationships between functional traits and prey specialization. A
⁴⁹ siphonophore is a colony bearing many feeding polyps (Fig. 1), each with a single tentacle,
⁵⁰ which branches into several tentilla carrying the functional cnidocytes (specialized neural cells

51 carrying nematocysts, the stinging capsules). Unlike most other cnidarians, siphonophores
52 carry their tentacle nematocysts in extremely complex and organized batteries (Skaer 1988)
53 built into their tentilla. While nematocyst batteries and clusters in other cnidarians are simple
54 static scaffolds for cnidocytes, siphonophore tentilla have their own reaction mechanism,
55 triggered upon encounter with prey. When it fires, a tentillum undergoes an extremely
56 fast conformational change that wraps it around the prey, maximizing the surface area
57 of contact for nematocysts to fire on the prey (Mackie et al. 1987). In addition, some
58 species have elaborate fluorescent and bioluminescent lures on their tentilla to attract prey
59 with aggressive mimicry (Purcell 1980; Haddock et al. 2005; Haddock and Dunn 2015).
60 Siphonophores bear four major nematocyst types in their tentacles and tentilla. The largest
61 type, heteronemes, have open-tip tubules characterized by bearing a distinctly wider spiny
62 shaft at the proximal end of the everted tubule. These are typically found flanking the
63 proximal end of the cnidoband. The most abundant type, haplonemes, have no distinct shaft,
64 but similarly to heteronemes, their tubules have open tips and can be found in the cnidoband.
65 Both heteronemes and haplonemes bear short spines along the tubule and can be toxic and
66 penetrate the surface of some prey types. In the terminal filament, siphonophores bear two
67 other types of nematocysts, characterized by their adhesive function, closed tip tubules, and
68 lack of spines on the tubule. These are the desmonemes (a type of adhesive coiled-tubule
69 spironeme), and rhopalonemes (a siphonophore-exclusive nematocyst type with wide tubules).

70 Many siphonophore species inhabit the deep pelagic ocean, which spans from ~200m to
71 the oceanic seafloor. This habitat has fairly homogeneous physical conditions and stable
72 zooplankton abundances and composition (Robison 2004). With a relatively predictable
73 prey availability, ecological theory would predict evolution to drive coexisting siphonophore
74 lineages towards specialization, increasing their feeding efficiencies and reducing interspecific
75 competition (Simpson 1944; Hardin 1960; Hutchinson 1961). If this prediction holds true,
76 we expect the prey capture apparatus morphologies of siphonophores to diversify with the
77 evolution of increased specialization on a variety of prey types in different siphonophore

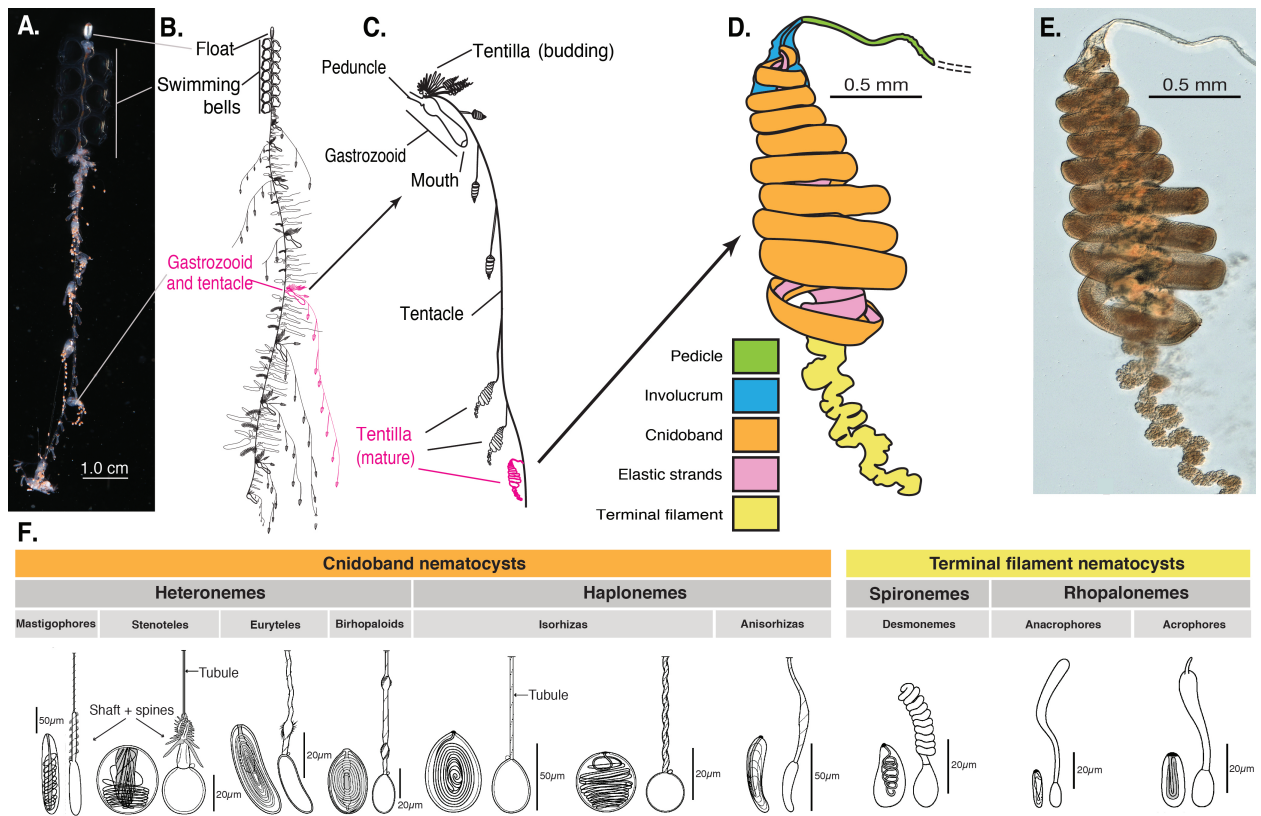


Figure 1: Siphonophore anatomy. A - *Nanomia* sp. siphonophore colony (photo by Catriona Munro). B,C - Illustration of a *Nanomia* colony, gastrozooid, and tentacle (by Freya Goetz). D - *Nanomia* sp. Tentillum illustration and main parts. E - Differential interference contrast micrograph of the tentillum illustrated in D. F - Nematocyst types (illustration reproduced with permission from Mapstone 2014), hypothesized homologies, and locations in the tentillum. Undischarged to the left, discharged to the right.

78 lineages.

79 Specialization is often thought to be an evolutionary ‘dead end’, meaning that specialized
80 lineages are unlikely to evolve into generalists or to shift the resource for which they are
81 specialized (Futuyma and Moreno 1988). However, recent studies have found that interspecific
82 competition can favor the evolution of resource generalism (Stireman-III 2005; Johnson et
83 al. 2009) and resource switching (Hoberg and Brooks 2008). Here we examine three
84 alternative hypotheses on siphonophore trophic specialization: (1) predatory specialists
85 evolved from generalist ancestors; (2) predatory specialists evolved from ancestral predators
86 which specialized on a different resource, switching their primary prey type; and (3) predatory
87 generalists evolved from specialist ancestors.

88 The study of siphonophore tentilla and diets has been limited in the past due to the
89 inaccessibility of their oceanic habitat and the difficulties associated with the collection of
90 fragile siphonophores. Thus, the morphological diversity of tentilla has only been characterized
91 for a few taxa, and their evolutionary history remains largely unexplored. Contemporary
92 underwater sampling technology provides an unprecedented opportunity to explore the trophic
93 ecology (Choy et al. 2017) and functional morphology (Costello et al. 2015) of siphonophores.
94 In addition, well-supported phylogenies based on molecular data are now available for these
95 organisms (Munro et al. 2018). These advances allow for the examination of relationships
96 between modern siphonophore form, function, and ecology, as well as reconstructing their
97 evolutionary history.

98 The few pioneering studies that have addressed the relationships between tentilla and
99 diet suggest that siphonophores are a robust system for the study of predatory specialization
100 via morphological diversification. (Purcell 1984) and (Purcell and Mills 1988) showed clear
101 relationships between diet, tentillum, and nematocyst characters in co-occurring epipelagic
102 siphonophores. These correlations, while studied for a small subset of extant epipelagic
103 siphonophore species, might be generalizable to all siphonophores. We hypothesize that
104 these relationships reflect correlated evolution between prey selection and tentillum (and

¹⁰⁵ nematocyst) traits. Furthermore, we hypothesize that with an extensive characterization of
¹⁰⁶ tentilla morphology, we can generate hypotheses about the diets of understudied siphonophore
¹⁰⁷ species.

¹⁰⁸ In this study, we characterize the morphological diversity of tentilla and their nematocysts
¹⁰⁹ across a broad variety of shallow and deep sea siphonophore species using modern imaging
¹¹⁰ technologies, we expand the phylogenetic tree of siphonophores by combining a broad taxon
¹¹¹ sampling of ribosomal gene sequences with a transcriptome-based backbone tree, and we
¹¹² explore the evolutionary histories and correlations among diet, tentillum, and nematocyst
¹¹³ characters.

¹¹⁴ Results

¹¹⁵ *Phylogeny* – Only 5 nodes (blue dots in Figure 3) in the unconstrained inference were
¹¹⁶ incongruent with the (Munro et al. 2018) transcriptome tree, and these were constrained
¹¹⁷ during estimation of the 18S+16S tree. The topology of the constrained tree presented here
¹¹⁸ (Fig. 3) is congruent with the resolved nodes in (Dunn et al. 2005) and (Munro et al. 2018).

¹¹⁹ We retained the clade nomenclature defined in (Dunn et al. 2005) and (Munro et al.
¹²⁰ 2018), such as Codonophora to indicate the sister group to Cystonectae, Euphysonectae to
¹²¹ indicate the sister group to Calycophorae, Clade A and B to indicate the two main lineages
¹²² within Euphysonectae. In addition, we define two new clades within Codonophora (Fig. 3):
¹²³ Eucladophora as the clade containing *Agalma elegans* and all taxa that are more closely related
¹²⁴ to it than to *Apolemia lanosa*, and Tendiculophora as the clade containing *Agalma elegans* and
¹²⁵ all taxa more closely related to it than to *Bargmannia elongata*. Eucladophora is characterized
¹²⁶ by bearing spatially differentiated tentilla with proximal heteronemes and a narrower terminal
¹²⁷ filament region. The etymology derives from the Greek *eu+kládos+phóros* for “true branch
¹²⁸ bearers”. Tendiculophora are characterized by bearing rhopalonemes and desmonemes in the
¹²⁹ terminal filament, having a pair of elastic strands, and developing proximally detachable
¹³⁰ cnidobands. The etymology of this clade is derived from the Latin *tendicula* for “snare or

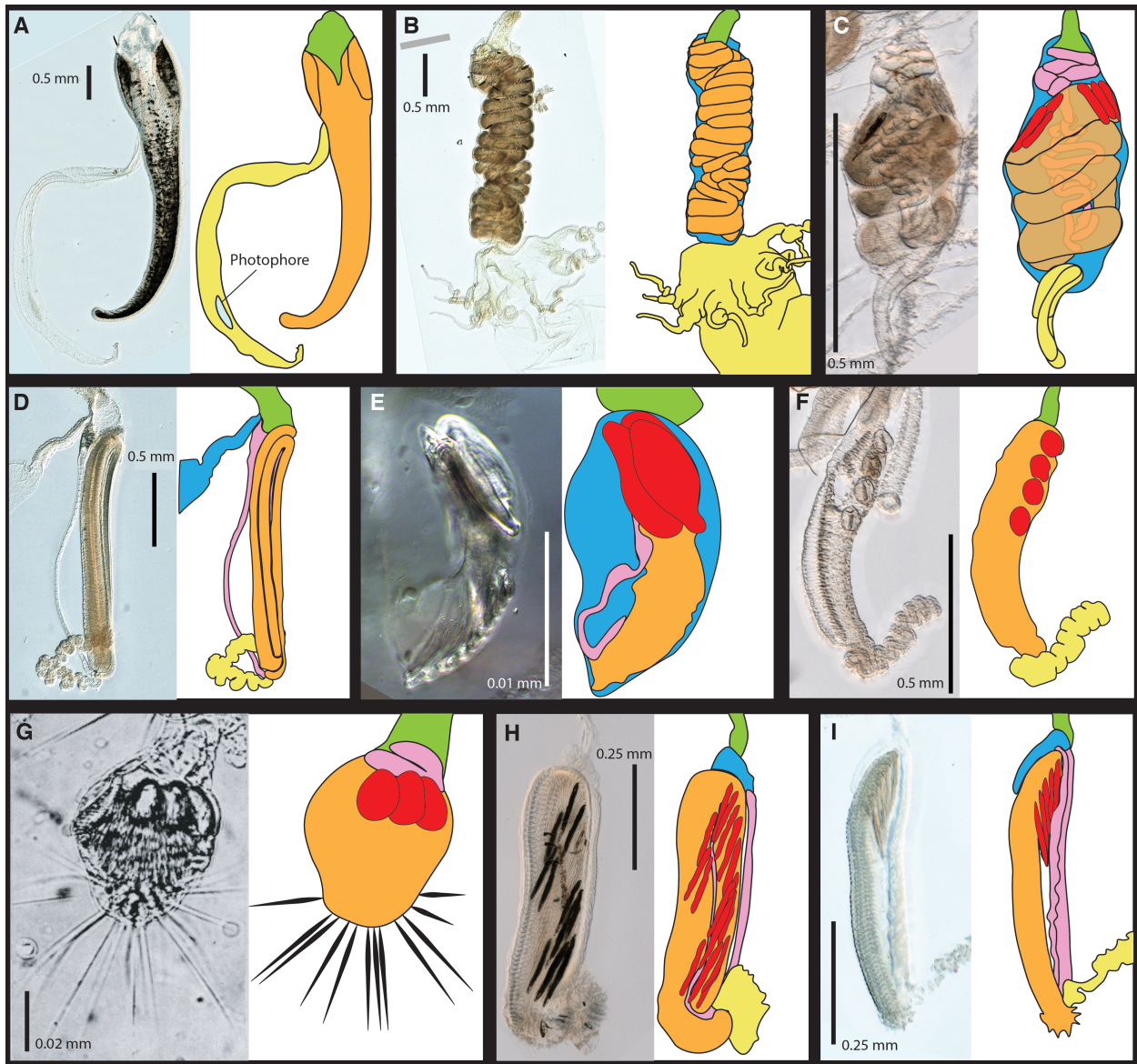


Figure 2: Tentillum diversity plate. The illustrations delineate the pedicle (green), involucrum (blue), cnidoband (orange), elastic strands (pink), terminal structures (yellow). Heteroneme nematocysts (stenoteles in C,E,F,G and mastigophores in H,I) are depicted in red for some species. A - *Erenna laciniata*, 10x. B - *Lychnagalma utricularia*, 10x. C - *Agalma elegans*, 10x. D - *Resomia ornicephala*, 10x. E - *Frillagalma vityazi*, 20x. F - *Bargmannia amoena*, 10x. G - *Cordagalma* sp., reproduced from Carré 1968. H - *Lilyopsis fluoracantha*, 20x. I - *Abylopsis tetragona*, 20x.

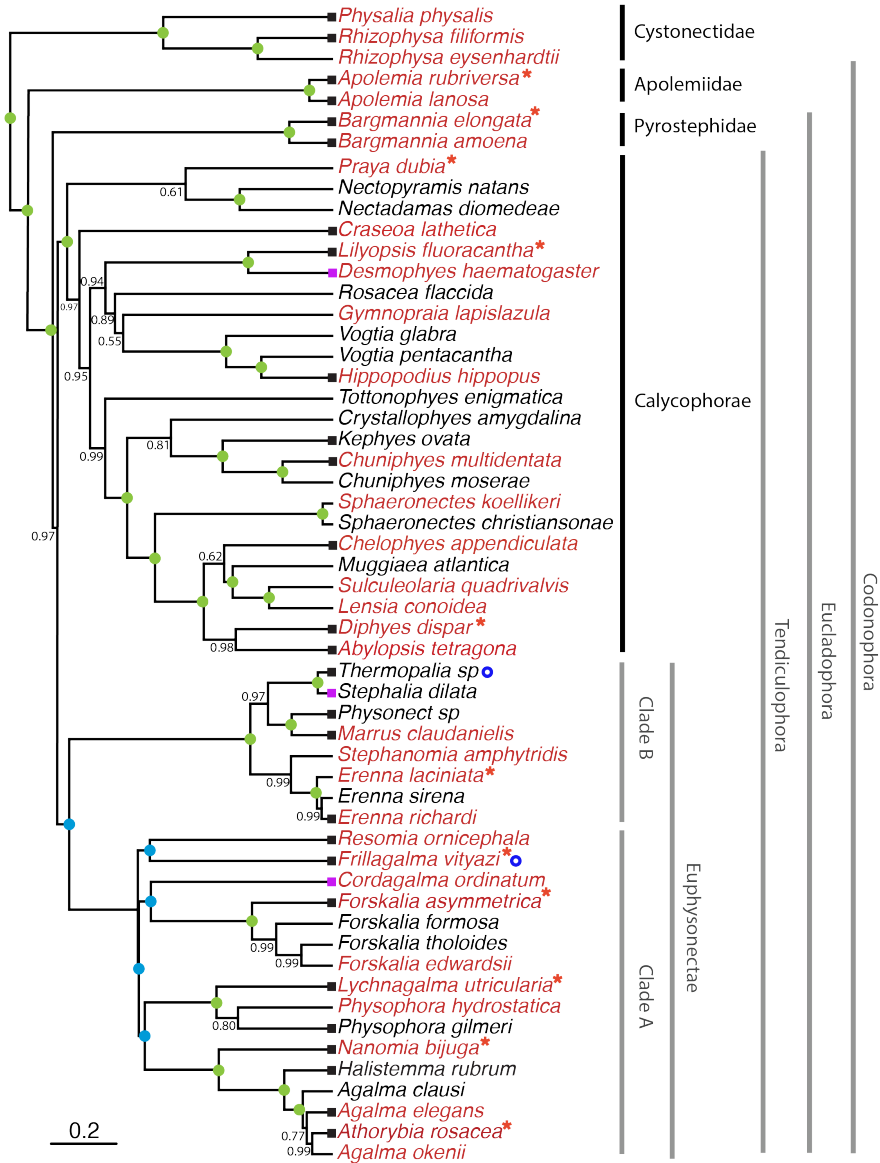


Figure 3: Bayesian time-tree built from 18S + 16S concatenated sequences. Branch lengths estimated using relaxed molecular clock. Species names in red indicate replicated representation in the morphology data. Species marked with a red asterisk were recorded using high speed video. Newly accessioned 16S data was used for species marked with a blue circle. Nodes labeled with Bayesian posteriors (BP). Green circles indicate BP = 1. Blue circles indicate nodes constrained to be congruent with (Munro *et al.* 2018). This phylogeny expands the taxon sampling of the (Munro *et al.* 2018) transcriptome tree and is congruent with it. Tips with black squares indicate the species with transcriptomes used in (Munro *et al.* 2018). Tips with grey squares indicate genus-level correspondence to taxa included in (Munro *et al.* 2018). The main clades are labeled: in black for described taxonomic units, and in grey for operational phylogenetic designations.

¹³¹ noose” and the Greek *phóros* for “carriers”.

¹³² *Evolutionary dynamics between diet and tentillum morphology* – Reconstructions of feeding
¹³³ guilds shows that generalism is not likely to be ancestral, and it appears to have evolved at
¹³⁴ least two times independently (Fig. 4). Large crustacean specialists evolve into generalists
¹³⁵ twice independently, supporting hypothesis 3. Feeding guild specializations have shifted
¹³⁶ from an alternative ancestral state at least five times, supporting hypothesis 2. Copepod
¹³⁷ specialization and fish specialization evolved twice, and ostracod specialization evolved at
¹³⁸ least once.

¹³⁹ The OUwie model comparison shows that out of 30 characters, 10 show significantly
¹⁴⁰ stronger support for the diet-driven multi-optima multi-rate OU model (SM15). These
¹⁴¹ characters include terminal filament nematocyst size and shape, involucrum length, elastic
¹⁴² strand width, and heteroneme number. Most of these characters are found exclusively in
¹⁴³ Tendiculophora, thus this may reflect processes that could be unique to this subtree. Five
¹⁴⁴ characters including cnidoband length, cnidoband shape, and haploneme length show maximal
¹⁴⁵ support for a diet-driven single-optimum OU model. The remaining 15 characters support
¹⁴⁶ BM (or OU with marginal AICc difference with BM).

¹⁴⁷ Phylogenetic logistic regressions identified evolutionary associations between individual
¹⁴⁸ characters and the presence of particular prey types in the diet (Fig. 4, right). Shifts toward
¹⁴⁹ ostracod presence in diet correlated with reductions in pedicle width and total haploneme
¹⁵⁰ volume. Shifts to copepod presence in the diet were associated with reductions in haploneme
¹⁵¹ width, cnidoband length and width, total haploneme and heteroneme volumes, and tentacle
¹⁵² and pedicle widths. Consistently, transitions to decapod presence in the diet correlated with
¹⁵³ more coiled cnidobands (SM21).

¹⁵⁴ Phylogenetic regressions of continuous characters against prey selectivity data produced
¹⁵⁵ additional insights. Fish selectivity is associated with increased number of heteronemes
¹⁵⁶ per tentillum, increased roundness of nematocysts (desmonemes and haplonemes), larger
¹⁵⁷ heteronemes, reduced heteroneme/cnidoband length ratios, smaller rhopalonemes, lower

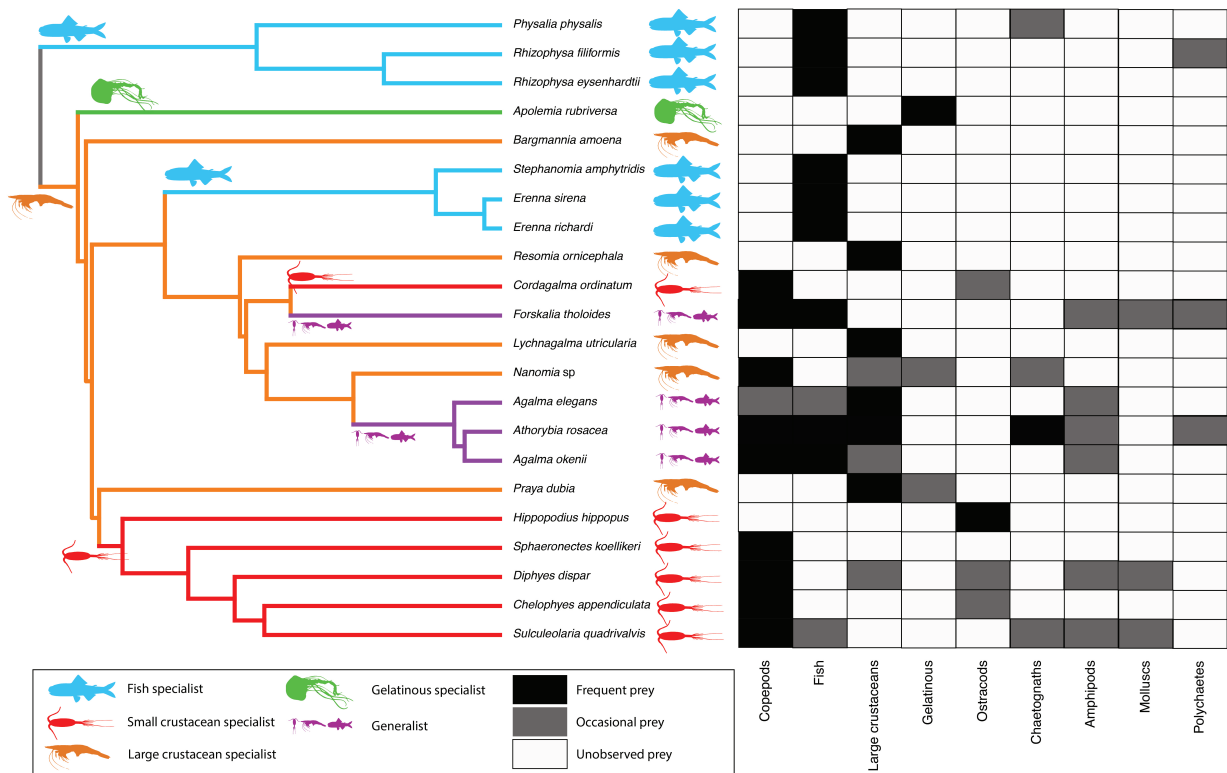


Figure 4: Left - Subset phylogeny showing the mapped feeding guild regimes that were used to inform the *OUwie* analyses. Right - Grid showing the prey items consumed from which the feeding guild categories were derived. Diet data were obtained from the literature review, available in the Dryad repository.

158 haploneme SA/V ratios, and increased size of the cnidoband, elastic strand, pedicle and
159 tentacle widths. Decapod-selective diets were associated with increasing cnidoband size and
160 coiledness, haploneme row number, elastic strand width, and heteroneme number. Copepod-
161 selective diets evolved in association with smaller heteroneme and total nematocyst volumes,
162 smaller cnidobands, rounder rhopalonemes, elongated heteronemes, narrower haplonemes
163 with higher SA/V ratios, and smaller heteronemes, tentacles, pedicles and elastic strands.
164 Selectivity for ostracods was associated with reductions in size and number of heteroneme
165 nematocysts, reductions in cnidoband size, number of haploneme rows, heteroneme number,
166 and cnidoband coiledness. Heteroneme length and elongation also correlated negatively with
167 chaetognath selectivity.

168 When some of the diet-morphology associations reported in the literature (Purcell 1984;
169 Purcell and Mills 1988) were tested for correlated evolution (Table 1), we found that most
170 were consistent with an evolutionary explanation except the relationship between terminal
171 filament nematocysts (rhopalonemes and desmonemes) and crustaceans in the diet. The latter
172 is likely a product of the larger species richness of crustacean-eating species with terminal
173 filament nematocysts, rather than simultaneous evolutionary gains.

174 Table 1. Tests of correlated evolution between morphological characters and aspects of
175 the diet found correlated in the literature.

Character	Aspect of diet	Test of evolutionary association	Relationship sign	P-value	Number of taxa	Association first report
Differentiated cnidobands	Hard bodied prey	Pagel's test	+	0.017	19	Purcell, 1984
Heteroneme volume	Copepod prey size	pGLS	+	0.002	8	Purcell, 1984
Terminal filament nematocysts	Crustacean diet	Pagel's test	Non-Significant	0.200	19	Purcell & Mills, 1988
Number of nematocyst types	Soft-bodied prey	Phylogenetic logistic regression	-	0.040	22	Purcell & Mills, 1988

177
178 *Generating dietary hypotheses using tentillum morphology* – The discriminant analysis of
179 principal components for feeding guild (7 principal components, 4 discriminants) produced
180 100% discrimination, and the highest loading contributions were found for the characters
181 (ordered from highest to lowest): Involucrum length, heteroneme volume, heteroneme number,
182 total heteroneme volume, tentacle width, heteroneme length, total nematocyst volume,

183 and heteroneme width (SM21). We used the predictions from this discriminant function
 184 to generate hypotheses about the feeding guild of 45 species in our morphological data
 185 (SM2). This projection predicts that two other *Apolemia* species may also be gelatinous prey
 186 specialists like *Apolemia rubriversa*, and that *Erenna laciniata* may be a fish specialist like
 187 *Erenna richardi*.

188 Table 2. Discriminant analysis of principal components for the presence of specific prey
 189 types using the morphological data. Top quartile variable (character) contributions to the
 190 linear discriminants are ordered from highest to lowest. Logistic regressions and GLMs
 191 were fitted to predict prey type presence and selectivity respectively. The sign of the slope
 192 of each predictor is reported, marked with an asterisk if significant (p value < 0.05), and
 193 highlighted grey if it differs between prey presence in diet and prey selectivity. Pseudo- R^2
 194 (%) approximates the percent variance explained by the model.

Prey type	DAPC	GLM for prey type presence (22 taxa)		Best fitting GLM for prey type selectivity (Purcell, 1981) (7 taxa)	
		Discrimination (%)	Top quartile variable contributions	Sign	Pseudo- R^2 (%)
Copepods	95.4	Total nematocyst volume	-	-*	
		Tentacle width	-	+	
		Haploneme elongation	-	+	
		Haploneme surface area/volume ratio	+		
		Haploneme row number	+	+	
		Cnidoband length	-	+	
		Cnidoband width	-	-	
Fish	68.1	Cnidoband free length	+	+	
		Total haploneme volume	-	+	
		Heteroneme volume	+	-	
		Total nematocyst volume	-	+	
		Total heteroneme volume	-	-	
		Cnidoband length	-	-	
		Cnidoband free length	+	+	
Large crustaceans	81.8	Involucrum length	-	-	
		Pedicle width	+	+	
		Involucrum length	+	+	
		Total heteroneme volume	-	-	
		Elastic strand width	-	+	
		Rhopaloneme length	+	+	
		Heteroneme volume	+	-	

195

196 *Phenotypic integration of the tentillum* – The quantitative characters we measured from
 197 tentilla and their nematocysts are highly correlated. The results indicate that the dimen-
 198 sionality of tentillum morphology is low, that many traits are associated with size, but that

199 nematocyst arrangement and shape are independent of it. The variance covariance matrices
200 (SM36-38) are congruent with the abundant positive correlations observed among simple
201 measurement characters in SM3. However, this analysis reveals more clearly the diagonal
202 blocks that constitute the evolutionary modules, such as the heteroneme block, the terminal
203 filament nematocyst block, and the cnidoband-pedicle-tentacle block. These results were
204 not very sensitive to transformation of inapplicable states and taxon sampling. When we
205 compared the rate covariance terms between characters across the different feeding guild
206 regimes (SM41), we found that half (48%) of the character pairs presented distinct correlation
207 coefficients across different regimes, indicating that the mode of phenotypic integration may
208 also shift with trophic niche. When contrasting the regime-specific rate correlation matrices
209 to the whole-tree matrix, we were able to identify the character dependencies that are unique
210 to each predatory niche (SM42).

211 Under the majority of SIMMAP outcomes, large crustaceans specialists are the first regime
212 to appear, and other regimes evolve in a shift from this ancestral specialization. Compared
213 to the rate correlation matrix estimated over the whole tree, large crustacean specialists
214 present strong negative correlations between haploneme elongation and heteroneme size,
215 and between rhopaloneme elongation and tentillum size, as well as with involucrum length.
216 With the appearance of generalists (*Forskalia* and the *Agalma-Athorybia* clade), terminal
217 filament nematocyst (desmonemes and rhopalonemes) sizes became negatively correlated with
218 the sizes of most characters, meaning that as some tentilla became larger, their individual
219 terminal nematocysts became smaller, observed to the extreme in *Agalma*. In addition,
220 heteroneme and rhopaloneme elongation became positively correlated with cnidoband size.
221 When large crustacean specialists switched to small crustacean prey in *Cordagalma* and
222 calycophorans, haploneme size became inversely correlated with heteroneme elongation,
223 which in turn developed a strong positive relationship with tentillum size. In other words, as
224 tentilla get smaller in this group, heteronemes get shorter and haplonemes get larger. The
225 extremes of this gradient can be seen in *Cordagalma* and *Hippopodius*. With the evolution

226 of fish prey specialization in cystonects and within Clade B, haploneme elongation became
227 negatively correlated with heteroneme elongation (signal driven by Clade B, since cystonects
228 lack tentacular heteronemes), and the surface area to volume ratio of haploneme nematocysts
229 switched from a strong negative relationship with cnidoband size (found in every other
230 regime) to a positively correlation. Gelatinous specialization, albeit appearing only once in
231 our tree, also carries a unique signature in character rate correlation shifts, with an increase
232 in the strength of the correlation between heteroneme shape and shaft width, consistent with
233 the appearance of birhopaloid nematocysts with swollen shafts that are likely effective at
234 anchoring gelatinous tissue (see reference to Narcomedusae nematocysts in (Purcell and Mills
235 1988)).

236 The phylogenetic positions of the main categorical character shifts were reconstructed
237 using stochastic character mapping (SM), and summarized in 5. Haploneme nematocysts are
238 likely ancestrally present in siphonophore tentacles, since they are present in the tentacles of
239 many other hydrozoans. Haplonemes first diverged into spherical isorhizas of 2 size classes
240 in Cystonectae, and elongated anisorhizas of one size class in Codonophora. Haplonemes
241 were likely lost in the tentacles of *Apolemia*, but spherical isorhizas are retained in other
242 *Apolemia* tissues (Siebert et al. 2013). Similarly, while heteronemes exist in other tissues
243 of cystonects, they appear in the tentacles of codonophorans exclusively, as birhopaloids in
244 *Apolemia*, ancestral stenoteles in eucladophoran physonects, and microbasic mastigophores in
245 calycophorans.

246 Eucladophora (the clade containing Pyrostephidae, Euphysonectae, and Calycophorae,
247 see main text Fig. 3) encompasses most of the extant Siphonophore species (178 of 186)
248 other than Cystonects and *Apolemia*. Innovations evolved in the stem of this group include
249 spatially segregated heteroneme and haploneme nematocysts, terminal filaments, and elastic
250 strands (Fig. 5). Pyrostephids evolved a unique bifurcation of the axial gastrovascular canal
251 of the tentillum known as the “saccus” (Totton and Bargmann 1965). The stem to the
252 clade Tendiculophora (clade containing Euphysonectae and Calycophorae, see main text

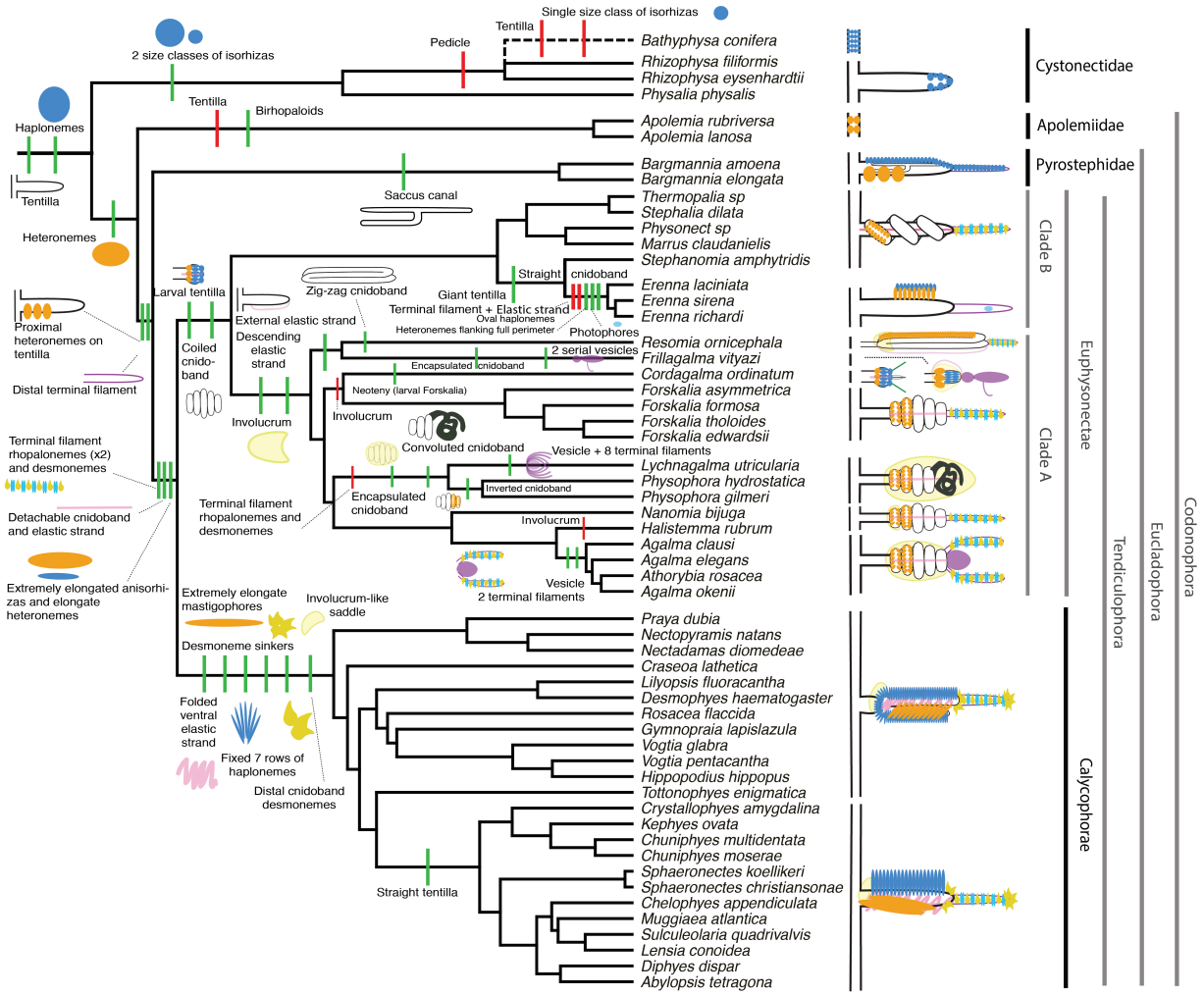


Figure 5: Siphonophore cladogram with the main categorical character gains (green) and losses (red) mapped. Some branch lengths were modified from the Bayesian chronogram to improve readability. The main visually distinguishable tentillum types are sketched next to the species that bear them, showing the location and arrangement of the main characters. In large, complex-shaped euphysonect tentilla, haplonemes were omitted for simplification. The rhizophysid *Bathyphysa conifera* branch was appended manually as a polytomy (dashed line).

253 Fig. 3) subsequently acquired further novelties such as the desmoneme and rhopaloneme
254 (acrophore subtype ancestral) nematocysts on the terminal filament (Fig. 5), which bears
255 no other nematocyst type (main text Fig. 1). These are arranged in sets of 2 parallel
256 rhopalonemes for each single desmoneme (Skaer 1988, 1991). The involucrum is an expansion
257 of the epidermal layer that can cover part or all of the cnidoband (main text Fig. 2). This
258 structure, together with differentiated larval tentilla, appeared in the stem branch to Clade
259 A physonects. Calycophorans evolved novelties such as larger desmonemes at the distal
260 end of the cnidoband, pleated pedicles with a “hood” (here considered homologous to the
261 involucrum) at the proximal end of the tentillum, anacrophore rhopalonemes, and microbasic
262 mastigophore-type heteronemes. While calycophorans have diversified into most of the extant
263 described siphonophore species (108 of 186), their tentilla have not undergone any major
264 categorical gains or losses since their most recent common ancestor. Nonetheless, they have
265 spread over a broad span of variation in nematocyst and cnidoband sizes.

266 *Evolution of nematocyst shape* – Haploneme nematocyst evolution has been mainly driven
267 by a single large shift towards elongation in Tendiculophora, which contains the majority of
268 described siphonophore species other than Cystonects, *Apolemia*, and Pyrostephidae. There
269 is one secondary return to more oval, less elongated haplonemes in *Erenna*, but it does not
270 reach the sphericity present in Cystonectae or Pyrostephidae (Fig. 6. Heteroneme evolution
271 presents a less discrete evolutionary history, where Tendiculophora evolved more elongate
272 heteronemes, but the difference between theirs and other siphonophores is much smaller than
273 the variation in shape within Tendiculophora, bearing no phylogenetic signal. In this clade,
274 evolution of heteroneme shape has diverged in both directions, and there is no correlation
275 with haploneme shape (Fig. 6), which has remained fairly constant (elongation between 1.5
276 and 2.5).

277 Haploneme and heteroneme shape share 21% of their variance across extant values,
278 and 53% of variance in their shifts along the branches of the phylogeny. However, much
279 of this correlation is due to the contrast between Pyrostephidae and their sister group

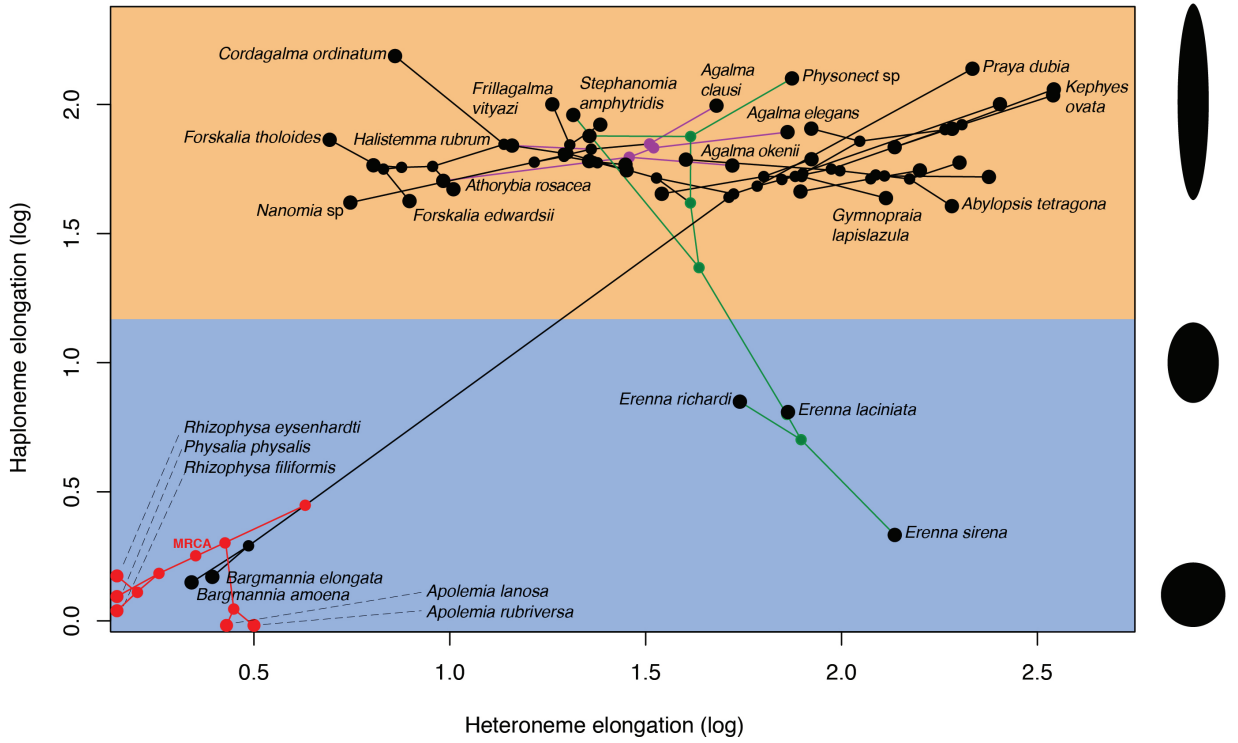


Figure 6: Phylomorphospace showing haploneme and heteroneme elongation (log scaled). Orange area delimits rod-shaped haplonemes, blue area covers oval and round shaped haplonemes. Smaller dots and lines represent phylogenetic relationships and ancestral states of internal nodes under BM. Species nodes in red were manually added to the plot. Cystonects have no tentacle heteronemes and are projected onto the haploneme axis. Apolemiids have no tentacle haplonemes and are projected onto the heteroneme axis. Colored branches and nodes correspond to BAMM regimes of accelerated haploneme shape (green) and heteroneme shape (violet) evolution.

280 Tendiculophora (Fig. 3). BAMM identified a regime shift in heteroneme shape evolution on
281 the branches leading to *Agalma* and *Athorybia*. For the rates of haploneme shape evolution,
282 BAMM identified two main independent regime shifts (Fig. 6): one in the branch leading
283 to Codonophora (anisorhizas diverging from cystonects' spherical isorhizas), and one in the
284 branch leading to Clade B physonects. Clade B includes *Erenna*, *Stephanomia*, *Marrus*, and
285 rhodaliids. Most of these taxa have rod-shaped anisorhizas, but *Erenna* has oval ones). No
286 clear regime shift patterns were identified in the evolution of desmoneme and rhopaloneme
287 shape.

288 Discussion

289 The core aims of this study are to examine the evolutionary history of siphonophore tentilla and
290 diet, characterize the evolutionary shifts in their trophic niches, and identify the morphological
291 characters that evolve with changes in prey type. We inquire whether the relationships between
292 form and function observed in extant taxa are due to correlated evolution or non-evolutionary
293 causes, whether the evolution of their trophic specializations supports or challenges traditional
294 ecological theory (such as the idea specialists evolve from generalists), and whether the diets
295 of siphonophores can be hypothesized by observing their tentacles. In addition, we produced
296 novel findings on tentillum morphology, siphonophore phylogeny, nematocyst character
297 evolution, and tentillum discharge dynamics.

298 *Evolution of tentillum morphology with diet* – Siphonophores are an abundant group of
299 zooplankton in oceanic ecosystems (Longhurst 1985; O'Brien 2007). While little is known
300 about siphonophore trophic ecology, what is known indicates that they occupy a central
301 position in midwater food webs (Choy et al. 2017), serving as trophic intermediaries between
302 smaller zooplankton and higher trophic level predators. Siphonophore species have been
303 observed to feed on a variety of prey with very different sizes, traits, and behaviors. Because
304 there is a total absence of siphonophores in the fossil record, how they became established
305 as the ubiquitous and diversified predators in today's oceans remains an open question.

306 Predators that use morphologically similar tools for prey capture tend to capture similar prey,
307 thus their abundance and coexisting species diversity are inversely related due to competitive
308 exclusion by resource limitation (Schluter 2000). However, this is not consistent with what
309 we observe in siphonophores, which have been found to be both very abundant and locally
310 diverse (Longhurst 1985, @mapstone2014global). We hypothesize that siphonophores have
311 escaped this by specializing on different prey resources.

312 According to our reconstructions, the evolutionary history of siphonophore diets indicates
313 that being a specialist was an ancestral aspect of their trophic niche, while trophic generalism
314 is likely a derived condition. Several studies (reviewed in (Futuyma and Moreno 1988))
315 have suggested that resource specialization is an irreversible dead end due to the constraints
316 posed by phenotypic specialization. Our reconstructions show that this is not the case for
317 siphonophores, where the prey type on which they specialize has shifted at least 5 times, and
318 generalism has evolved independently at least twice. Among the evolutionary hypotheses
319 considered, we find support for both hypotheses 2 (specialist resource switching) and 3
320 (specialist to generalist), but no support for hypothesis 1 (generalist to specialist). This is
321 consistent with the findings of recent studies on phytophagous insects (Nosil 2002), where the
322 rate of evolution from generalists to specialists is comparable to the reverse, thus specialization
323 does not limit further evolution. However, (Nosil and Mooers 2005) found that ancestral
324 reconstruction methods can be biased, and tend to infer higher transition rates toward the
325 more frequent state. With this in mind, we should expect to find a predominance of transitions
326 from generalists to specialists (the more common state across the tips). Nonetheless, we
327 observe the opposite, indicating strong evidence that these generalists are indeed a derived
328 state. Our results are also consistent with (Hardy and Otto 2014)'s study on lepidopterans,
329 where specialized resource switching is the primary transition type while niche breadth remains
330 fairly constant. The evolutionary history of tentilla shows that siphonophores are an example
331 of trophic niche diversification via morphological innovation and evolution, which allowed
332 transitions between specialized trophic niches. This strategy is particularly important in a

³³³ deep open ocean ecosystem, which is a relatively homogeneous physical environment, where
³³⁴ the primary niche heterogeneity available is the potential interactions between organisms
³³⁵ (Robison 2004).

³³⁶ One of the most common prey items found in siphonophore diets is copepods (Fig. 4).
³³⁷ Copepod-specialized diets have evolved convergently in *Cordagalma* and some calycophorans.
³³⁸ These evolutionary transitions happened together with transitions to smaller tentilla with
³³⁹ fewer cnidoband nematocysts. Tentilla are expensive single-use structures, therefore we would
³⁴⁰ expect that specialization in small prey would beget reductions in the size of the prey capture
³⁴¹ apparatus to the minimum required for the ecological performance. *Cordagalma*'s tentilla
³⁴² strongly resemble the larval tentilla (only found in the first-budded feeding body of the
³⁴³ colony) of their sister genus *Forskalia* spp. This indicates that the evolution of *Cordagalma*
³⁴⁴ tentilla could be a case of paedomorphosis associated with predatory specialization on smaller
³⁴⁵ prey.

³⁴⁶ (Purcell 1984) showed that haplonemes have a penetrating function as isorhizas in
³⁴⁷ cystonects and an adhesive function as anisorhizas in Tendiculophora. The two clades that
³⁴⁸ have been observed primarily feeding on fish (Cystonectae and Clade B, which includes
³⁴⁹ *Erenna*, *Stephanomia*, *Marrus*, and rhodaliids) present an accelerated rate of haploneme
³⁵⁰ shape evolution towards more compact haplonemes, significantly distinct from their closest
³⁵¹ relatives. Isorhizas in cystonects are known to penetrate the skin of fish during prey capture,
³⁵² and to deliver the toxins that aid in paralysis and digestion (Hessinger 1988). *Erenna*
³⁵³ anisorhizas are also able to penetrate human skin and deliver a painful sting (Pugh 2001)
³⁵⁴ (and pers. obs.), a common feature of piscivorous cnidarians like cystonects or cubozoans.

³⁵⁵ (Thomason 1988) hypothesized that smaller, more spherical nematocysts, with a lower
³⁵⁶ surface area to volume ratio, are more efficient in osmotic-driven discharge and thus have
³⁵⁷ more power for skin penetration. The elongated haplonemes of crustacean-eating Tendicu-
³⁵⁸ lophora have never been observed penetrating their crustacean prey ((Purcell 1984) and our
³⁵⁹ unpublished observations), and are hypothesized to entangle the prey through adhesion of

360 the abundant spines to the exoskeletal surfaces and appendages. Entangling requires less
361 acceleration and power during discharge than penetration, as it does not rely on point pressure.

362 In fish-eating cystonects and *Erenna* species, the haplonemes are much less elongated and
363 very effective at penetration, in congruence with the osmotic discharge hypothesis.

364 When we tested the diet-morphology correlation hypotheses supported in the literature
365 from a macroevolutionary perspective (Table 1), we found that most of them were consis-
366 tent with correlated evolution. The ecomorphological association between rhopalonemes,
367 desmonemes, and crustacean eaters was not congruent with a scenario of correlated evolution.
368 This is probably due to the broader set of taxa in our analyses, including multiple species
369 without desmonemes or rhopalonemes but which effectively capture crustaceans (such as
370 *Cordagalma ordinatum*, *Lychnagalma utricularia*, and *Bargmannia amoena*).

371 Our work identifies an interesting example of convergent evolution. The region of the
372 tentillum morphospace (Supplementary Figure XX) occupied by calycophorans was indepen-
373 dently (and more recently) occupied by the physonect *Frillagalma vityazi*. Like calycophorans,
374 *Frillagalma* tentilla have small C-shaped cnidobands with a few rows of anisorhizas. Unlike
375 calycophorans, they lack paired elongate microbasic mastigophores. Instead, they bear three
376 elongated stenoteles, and their cnidobands are followed by a branched vesicle, unique to this
377 genus. Their tentillum morphology is very different from that of other related physonects,
378 which tend to have long, coiled, cnidobands with many paired oval stenoteles. Most studies
379 on calycophoran diets have reported their prey to be primarily composed of small crustaceans,
380 such as copepods or ostracods (Purcell 1981, 1984). The diet of *Frillagalma vityazi* is un-
381 known, but this morphological convergence suggests that they evolved to capture similar
382 kinds of prey. Our DAPCs (Supp. Fig XXX) predict that *Frillagalma* has a generalist niche
383 with both soft and hard bodied prey, including copepods.

384 While our results unambiguously show that tentillum morphology evolved with diet, the
385 conclusions we can draw from these analyses are limited by the sparse dietary data available.
386 Moreover, our analyses are not sufficient to adequately test hypotheses of adaptation, since

387 that would require evidence of changes within a population exposed to different selective
388 pressures. When interpreting these results, it is important to remember that diet is a product
389 of environmental prey availability and predator selectivity. Selectivity differences across
390 siphonophore species could be driven by other phenotypes not accounted for this study. For
391 example, tentacle-deploying behavior, positioning in the water column, sensitivity thresholds
392 for nematocyst discharge, or chemical cues to ingest a captured animal. Further observations
393 on these behaviors in the field are necessary to assess their relative importance in determining
394 dietary composition. In addition to behavior, there is much biochemistry in the prey capture
395 and digestion processes that remains unexplored. Part of the success in siphonophore prey
396 capture is likely determined by the effectiveness of the toxins delivered by the nematocysts
397 on different taxa. Comparative toxin assays and venom protein evolution studies would
398 shed light on this question. Moreover, siphonophore trophic specialization may have brought
399 changes in the digestive biochemistry of gastrozooids and palpons. A comparison of the gene
400 expression levels for different enzymes in the gastrozooids of different species, together with
401 digestive enzyme sequence evolution studies, and a toxicological assay of the different venoms
402 in siphonophore nematocysts on different prey taxa, would provide a great complement to
403 our results.

404 *Phenotypic integration of siphonophore tentilla* – Many tentillum characters, such as
405 nematocysts, arose from the subfunctionalization of serial homologs (David et al. 2008). Serial
406 homologs have shared genetic elements underlying their development, and are expected to
407 have phylogenetic correlations (Wagner and Schwenk 2000). In addition, these sub-structures
408 must fit and work together in synchrony to ensnare prey successfully (functional integration).
409 Character complexes that satisfy these conditions tend to be phenotypically integrated.
410 Phenotypic integration is the set of functional and genetic correlations among the traits of an
411 organism (Pigliucci 2003). These correlations have been hypothesized to direct and constrain
412 adaptive evolution (Wagner and Schwenk 2000). The siphonophore tentillum morphospace
413 has a fairly low extant dimensionality due to an evolutionary history with many synchronous,

⁴¹⁴ correlated changes. This is consistent with strong phenotypic integration where genetic and
⁴¹⁵ developmental correlations are maintained by natural selection to preserve function.

⁴¹⁶ Structural correlations within the tentillum are expected from shared regulatory networks
⁴¹⁷ within a common developmental bud (budding tentilla in the tentacle). Similarly, correlations
⁴¹⁸ between nematocyst subtypes are also expected given their common evolutionary and develop-
⁴¹⁹ mental origin. None of these explanations for correlated evolution are surprising, nor require
⁴²⁰ natural selection. However, we also found correlations between nematocyst and tentillum
⁴²¹ characters. Siphonophore tentacle nematocysts (in their cnidocytes) are not produced nor
⁴²² matured in the developing tentillum. These cnidocytes are produced by dividing cnidoblasts
⁴²³ in the basigaster (basal swelling of the gastrozooid). Once the cnidocytes have assembled the
⁴²⁴ nematocyst, they migrate outward along the tentacle (Carré 1972) and position themselves
⁴²⁵ in the tentillum according to their type and size (Skaer 1988). Thus, the developmental pro-
⁴²⁶ grams that produce the observed nematocyst morphologies are spatially separated from those
⁴²⁷ producing the tentillum morphologies. Therefore, we hypothesize the genetic correlations and
⁴²⁸ phenotypic integration between tentillum and nematocyst characters are maintained through
⁴²⁹ natural selection on separate regulatory networks, out of the necessity to work together and
⁴³⁰ meet the spatial, mechanical, and functional constraints of their prey capture behavior.

⁴³¹ Our evolutionary rate covariance results indicate that tentilla are not only phenotypically
⁴³² integrated, but also show patterns of evolutionary modularity, where different sets of characters
⁴³³ appear to evolve in stronger correlations among each other than with other characters. This
⁴³⁴ may be indicative of the underlying genetic and developmental dependencies among closely
⁴³⁵ homologous nematocyst types (such as desmonemes and rhopalonemes) and structures. In
⁴³⁶ addition, these evolutionary modules point to hypothetical functional modules. For example,
⁴³⁷ the coiling degree of the cnidoband and the extent of the involucrum have correlated rates of
⁴³⁸ evolution, while high speed videos show that the involucrum helps direct the whiplash of the
⁴³⁹ uncoiling cnidoband forward (towards the prey).

⁴⁴⁰ While selection acting on character states is a widely studied phenomenon, recent studies

441 have shown that selection can also act upon the patterns of character correlations and
442 phenotypic dependencies (Young and Hallgrímsson 2005; Goswami 2006; Revell and Collar
443 2009; Monteiro and Nogueira 2010; Hallgrímsson et al. 2012; Claverie and Patek 2013;
444 Caetano and Harmon 2018). This evolution of character relationships can allow lineages
445 to explore new regions of the morphospace and facilitate the appearance of ecological
446 novelties. Our results show that the patterns of phenotypic integration in siphonophore
447 tentilla vary among clades, and appear to display different relationships across shifting feeding
448 specializations. Similarly to what has been found in the feeding morphologies of fish (Collar
449 et al. 2005; Revell and Collar 2009), siphonophore tentilla may have accommodated new diets
450 by altering the correlations between characters. For example, changes in the size and shape
451 relationships between nematocyst types gave rise to the nematocyst complements specialized
452 in ensnaring small crustaceans or fish. Finally, the evolvability of phenotypic dependencies
453 likely had a large role in the evolution of the diverse tentilla morphologies we observe today
454 across siphonophores.

455 *Evolution of nematocyst shape* – The phylogenetic placement of siphonophores among the
456 Hydrozoa remains an unresolved question (Munro et al. 2018). The most recent work on
457 this front sets them as sister group to all other Hydroidolina (Kayal et al. 2015). Therefore,
458 there is a great uncertainty around the ancestral plesiomorphies of the common ancestor
459 of all siphonophores. This is especially true for those characters that present extreme
460 differences between Cystonectae and Codonophora (the earliest split in the siphonophore
461 phylogeny). One such character is the shape of haploneme nematocysts. A remarkable
462 feature of siphonophore haplonemes is that they are outliers to all other Medusozoa in
463 their surface area to volume relationships, deviating significantly from sphericity (Thomason
464 1988). This suggests a different mechanism for their discharge that could be more reliant on
465 capsule tension than on osmotic potentials (Carré and Carré 1980), and strong selection for
466 efficient nematocyst packing in the cnidoband (Thomason 1988; Skaer 1988). Our results
467 show that Codonophora underwent a shift towards elongation and Cystonectae towards

⁴⁶⁸ sphericity, assuming the common ancestor had an intermediate state. Since we know that
⁴⁶⁹ the haplonemes of other hydrozoan outgroups are generally spheroid, it is more parsimonious
⁴⁷⁰ to assume that cystonects retain this ancestral state. Later, we observe a return to more
⁴⁷¹ rounded (ancestral) haplonemes in *Erenna*, concurrent with a secondary gain of a piscivorous
⁴⁷² trophic niche, like that exhibited by cystonects.

⁴⁷³ The implications of these results to the evolution of nematocyst function are that an
⁴⁷⁴ innovation in the discharge mechanism of haplonemes may have occurred during the main shift
⁴⁷⁵ to elongation. Elongate nematocysts can be tightly packed into cnidobands. We hypothesize
⁴⁷⁶ this may be a Tendiculophora lineage-specific adaptation to packing more nematocysts into
⁴⁷⁷ a limited tentillum space, as suggested by (Skaer 1988). Tendiculophora, comprised of
⁴⁷⁸ the clades Euphysonectae and Calycophorae, includes the majority of siphonophore species.
⁴⁷⁹ Among these, are the most abundant siphonophore species, and a greater morphological and
⁴⁸⁰ ecological diversity is found. We hypothesize that this packing-efficient haploneme morphology
⁴⁸¹ may have been a key innovation leading to the diversification of this clade. However, other
⁴⁸² characters that shifted concurrently in the stem of this clade may have been responsible for
⁴⁸³ their extant diversity.

⁴⁸⁴ Conclusions

⁴⁸⁵ Siphonophores have diverse predatory niches in the open ocean, ranging from mid-trophic
⁴⁸⁶ small crustacean eaters to piscivorous super-carnivores. With the evolution of diversified
⁴⁸⁷ prey type specializations comes the evolution of morphologies adapted to the challenges
⁴⁸⁸ posed by different prey. The results presented here indicate that the associations found
⁴⁸⁹ between siphonophore tentilla and their prey are a product of correlated evolution in highly
⁴⁹⁰ integrated traits. While much of the literature focuses on how predatory generalists evolve
⁴⁹¹ into predatory specialists, in siphonophores we find predatory specialists can evolve into
⁴⁹² generalists, and that specialists on one prey type have directly evolved into specialists on
⁴⁹³ other prey types. Our extended morphological characterization shows that the relationships

494 between form and ecology hold across a large set of taxa and characters, and can be used
495 to generate hypotheses on the feeding habits of uncharacterized species. We find that the
496 evolutionary diversification of tools for prey capture contributed to the diversification of
497 trophic interactions. Therefore, we identify organismal trait evolution as a key driver in the
498 emergence of food web complexity.

499 Materials and Methods

500 *Tentillum morphology* – The morphological work was carried out on siphonophore specimens
501 fixed in 4% formalin from the Yale Peabody Museum Invertebrate Zoology (YPM-IZ) collection
502 (accession numbers in Dryad repository). These specimens were collected intact across many
503 years of fieldwork expeditions, using blue-water diving (Haddock and Heine 2005), remotely
504 operated vehicles (ROVs), and human-operated submersibles. Tentacles were dissected
505 from non-larval gastrozooids, sequentially dehydrated into 100% ethanol, cleared in methyl
506 salicylate, and mounted onto slides with Canada Balsam or Permount mounting media.
507 The slides were imaged as tiled z-stacks using differential interference contrast (DIC) on an
508 automated stage at YPM-IZ (with the assistance of Daniel Drew and Eric Lazo-Wasem) and
509 with laser point confocal microscopy using a 488 nm Argon laser that excited autofluorescence
510 in the tissues. Thirty characters (defined in SM5) were measured using Fiji (Collins 2007;
511 Schindelin et al. 2012). We did not measure the lengths of contractile structures (terminal
512 filaments, pedicles, gastrozooids, and tentacles), since they are too variable to quantify.
513 We measured at least one specimen for 96 different species (see raw data by species in
514 Dryad). Of these, we selected 38 focal species across clades based on specimen availability
515 and phylogenetic representation. Three to five tentacle specimens from each one of these
516 selected species were measured to capture intraspecific variation.

517 *Siphonophore phylogeny* – While the main goal of this work is not to elucidate a novel
518 phylogeny for Siphonophora, we did expand on the most recent transcriptome based phylogeny
519 (Munro et al. 2018) to accommodate a larger taxon sampling. In order to do this, we

520 ran a constrained analysis on an extensive 18S+16S dataset. The phylogenetic analysis
521 included 55 siphonophore species and 6 outgroup cnidarian species (*Clytia hemisphaerica*,
522 *Hydra circumcincta*, *Ectopleura dumortieri*, *Porpita porpita*, *Velella velella*, *Staurocladia*
523 *wellingtoni*). The gene sequences we used in this study are available online (accession numbers
524 in Dryad Repository). Some of the sequences we used were accessioned in (Dunn et al. 2005),
525 and others we extracted from the transcriptomes in (Munro et al. 2018). Two new 16S
526 sequences for *Frillagalma vityazi* (MK958598) and *Thermopalia* sp. (MK958599) sequenced
527 by Lynne Christianson using the primers from (Cunningham and Buss 1993) (read 3' to 5' F:
528 TCGACTGTTACCAAAACATAGC , R: ACGGAATGAACTCAAATCATGTAAG) were
529 included and accessioned to NCBI. We aligned these sequences using MAFFT (Katoh et al.
530 2002) (alignments available in Dryad). We inferred a Maximum Likelihood (ML) phylogeny
531 (SM6) from 16S and 18S ribosomal rRNA genes using IQTree (Nguyen et al. 2014) with
532 1000 bootstrap replicates (iqtree -s alignment.fa -nt AUTO -bb 1000). We used ModelFinder
533 (Kalyaanamoorthy et al. 2017) implemented in IQTree v1.5.5. to assess relative model fit.
534 ModelFinder selected GTR+R4 for having the lowest Bayesian Information Criterion score.
535 Additionally, we inferred a Bayesian tree with each gene as an independent partition in
536 RevBayes (Höhna et al. 2016) (SM9,SM11), which was topologically congruent with the
537 unconstrained ML tree. The *alpha* priors were selected to minimize prior load in site variation.

538 Given the broader sequence sampling of the transcriptome phylogeny, we ran constrained
539 inferences (using both ML and Bayesian timetree approaches, which produced fully congruent
540 topologies (SM8, SM10)) after fixing the 5 nodes that were incongruent with the topology
541 of the consensus tree in (Munro et al. 2018). This topology was then used to inform a
542 Bayesian relaxed molecular clock time-tree in RevBayes, using a birth-death process (sampling
543 probability calculated from the known number of described siphonophore species) to generate
544 ultrametric branch lengths (SM11,SM12). Scripts available in the Dryad repository.

545 *Feeding ecology* – We extracted categorical diet data for different siphonophore species
546 from published sources, including seminal papers (Biggs 1977; Purcell 1981, 1984; Andersen

547 1981; Mackie et al. 1987; Pugh and Youngbluth 1988; Bardi and Marques 2007), and
548 ROV observation data (Hissmann 2005; Choy et al. 2017) with the assistance of Elizabeth
549 Hetherington and C. Anela Choy (available in Dryad repository). We removed the gelatinous
550 prey observations for *Praya dubia* eating a ctenophore and a hydromedusa, and for *Nanomia*
551 sp. eating *Aegina*, since we believe these are rare events that have a much larger probability
552 of being detected by ROV methods than their usual prey, and it is not clear whether
553 the medusae were attempting to prey upon the siphonophores. Personal observations on
554 feeding (from SHDH, CAC, and Philip Pugh) were also included for *Resomia ornicephala*,
555 *Lychnagalma utricularia*, *Bargmannia amoena*, *Erenna richardi*, *Erenna laciniata*, *Erenna*
556 *sirena*, and *Apolemia rubriversa*. In order to detect coarse-level patterns in the feeding
557 habits, the data were merged into feeding guilds. The feeding guilds described here are:
558 small-crustacean specialist (feeding mainly on copepods and ostracods), large crustacean
559 specialist (feeding on large decapods, mysids, or krill), fish specialist (feeding mainly on
560 actinopterygian larvae, juveniles, or adults), gelatinous specialist (feeding mainly on other
561 siphonophores, medusae, ctenophores, salps, and/or doliolids), and generalist (feeding on
562 a combination of the aforementioned taxa, without favoring any one prey group). These
563 were selected to minimize the number of categories while keeping the most different types of
564 prey separate. We extracted copepod prey length data from (Purcell 1984). To calculate
565 specific prey selectivities, we extracted quantitative diet and zooplankton composition data
566 from (Purcell 1981), matched each diet assessment to each prey field quantification by
567 site, calculated Ivlev's electivity indices (Jacobs 1974), and averaged those by species (data
568 available in Dryad repository).

569 *Statistical analyses* – For subsequent comparative analyses, we removed species present in
570 the tree but not represented in the morphology data, and *vice versa*. Although we measured
571 specimens labeled as *Nanomia bijuga* and *Nanomia cara*, we are not confident in some of the
572 species-level identifications, and some specimens were missing diagnostic zooids. Thus, we
573 decided to collapse these into a single taxonomic concept (*Nanomia* sp.). All *Nanomia* sp.

574 observations were matched to the phylogenetic position of *Nanomia bijuga* in the tree. We
575 carried out all phylogenetic comparative statistical analyses in the programming environment
576 R (Team 2017), using the Bayesian ultrametric species tree (Fig. 3), and incorporating
577 intraspecific variation estimated from the specimen data as standard error whenever the
578 analysis tool allowed it. R scripts and summarized species-collapsed data available in the
579 Dryad repository. For each character (or character pair) analyzed, we removed species
580 with missing data and reported the number of taxa included. We tested each character for
581 normality using the Shapiro-Wilk test (Shapiro and Wilk 1965), and log-transformed those
582 that were non-normal.

583 We fitted different models generating the observed data distribution given the phylogeny for
584 each continuous character using the function fitContinuous in the R package *geiger* (Harmon
585 et al. 2007). The models compared were the white noise (WN; non-phylogenetic model that
586 assumes all values come from a single normal distribution with no covariance structure among
587 species), the Brownian Motion (BM) model of neutral divergent evolution (Martins 1996), the
588 Early Burst (EB) model of decreasing rate of evolutionary change (Harmon et al. 2010), and
589 the Ornstein-Uhlenbeck (OU) model of stabilizing selection around a fitted optimum state
590 (Uhlenbeck and Ornstein 1930; Butler and King 2004). We then ranked the models in order
591 of increasing parametric complexity (WN,BM,EB,OU), and compared the corrected Akaike
592 Information Criterion (AICc) support scores (Sugiura 1978) to the lowest (best) score, using
593 a cutoff of 2 units to determine significantly better support. When the best fitting model
594 was not significantly better than a less complex alternative, we selected the least complex
595 model (SM13). We calculated model adequacy scores using the R package *arbutus* (Pennell
596 et al. 2015) (SM14). We calculated phylogenetic signal in each of the measured characters
597 using Blomberg's K (Blomberg et al. 2003) (SM13). We reconstructed ancestral states using
598 Maximum Likelihood (R phytools::anc.ML (Revell 2012)), and stochastic character mapping
599 (R phytools::make.simmap) for categorical characters. R scripts available in Dryad.

600 In order to study the evolution of predatory specialization, we reconstructed components

601 of the diet and prey selectivity on the phylogeny using ML (R `phytools::anc.ML`). To identify
602 evolutionary associations of diet with tentillum and nematocyst characters, we compared the
603 performance of a neutral evolution model to that of a diet-driven directional selection model.
604 First, we collapsed the diet data into the five feeding guilds mentioned above (fish specialist,
605 small crustacean specialist, large crustacean specialist, gelatinous specialist, generalist), based
606 on which prey types they were observed consuming most frequently. Then, we reconstructed
607 the feeding guild ancestral states using the ML function `ace` (package `ape` (Paradis et al.
608 2019)), removing tips with no feeding data. The ML reconstruction was congruent with the
609 consensus stochastic character mapping (SM31). Then, using the package `OUwie` (Beaulieu
610 and O'Meara 2012), we fitted an OU model with multiple optima and rates of evolution
611 matched to the reconstructed ancestral diet regimes, a single optimum OU model, and a BM
612 null model, inspired by the analyses in (Cressler et al. 2015). Finally, we compared their
613 AICc support values to select the best fitting model (SM15).

614 To model the evolutionary associations between individual tentillum and nematocyst
615 characters and the ability to capture particular prey types in the diet, we ran a series of
616 phylogenetic generalized linear models (R `phylolm::phyloglm`) (SM21). In addition, we ran a
617 series of comparative analyses to address hypotheses of diet-tentillum relationships posed in
618 the literature. To test for correlated evolution among binary characters, we used Pagel's test
619 (Pagel 1994). To characterize and evaluate the relationship between continuous characters, we
620 used phylogenetic generalized least squares regressions (PGLS) (Grafen 1989). To compare
621 the evolution of continuous characters with categorical aspects of the diet, we carried out a
622 phylogenetic logistic regression (R `nlme::gls` using the 'corBrownian' function for the argument
623 'correlation').

624 In order to study correlations between the rates of evolution between different characters,
625 we fitted a set of evolutionary variance covariance matrices (Revell and Collar 2009) (R
626 `phytools::evol.vcv`). When fitting all covariance terms simultaneously (SM36-38), we selected
627 the largest set of characters that would allow the analysis to run without computational

628 singularities. This excluded many of the morphometric characters which are linearly dependent
629 on other characters. Since the functions do not tolerate missing data, we ran the analyses
630 in two ways: One including all taxa but transforming absent states to zeroes, and another
631 removing the taxa with absent states. To test whether phenotypic integration changes across
632 selective regimes determined by the reconstructed feeding guilds, we carried out character-
633 pairwise variance covariance analysis comparing alternative models (R phytools::evolcv.lite),
634 including those where correlations are the same across the whole tree and models where
635 correlations differ between selective regimes (SM42). These analyses could only be carried out
636 on the subset of taxa for which diet data is available, and only among character pairs that are
637 not computationally singular for that taxonomic subset. Finally, we compared regime-specific
638 variance covariance matrices to the general matrix and to their preceding regime matrix to
639 identify the changes in character dependence unique to each regime (SM43). Gelatinous
640 specialist correlations could only be estimated for a small subset of characters present in
641 *Apolemia*, and should be interpreted with care.

642 To generate hypotheses about the diets of understudied siphonophores for which no feeding
643 observations have yet been reported (but for which we have tentacle morphology data), we
644 carried out linear discriminant analysis of principal components (DAPC) using the dapc
645 function (R adegenet::dapc) (Jombart et al. 2010). This function allowed us to incorporate
646 more predictors than individuals. We generated discriminant functions for feeding guild,
647 soft/hard bodied prey, and for the presence of copepods, fish, and shrimp (large crustaceans)
648 in the diet (SM16-20). From these DAPCs we obtained the highest contributing morphological
649 characters to the discriminaton (characters in the top quartile of the weighted sum of the
650 linear discriminant loadings controlling for the eigenvalue of each discriminant). For each
651 DAPC we generated hypotheses about the diets of siphonophores outside the training set
652 (R adegenet::predict.dapc), incorporating prediction uncertainty as posterior probabilities
653 (SM16-20). In order to identify the sign of the relationship between the predictor characters
654 prey type presence in the diet, we then generated generalized logistic regression models (as

655 a type of generalized linear model, or GLM using R stats::glm) with the top contributing
656 characters (from the corresponding DAPC) as predictors. We also carried out these GLMs on
657 the Ivlev's selectivity indices for each prey type calculated from (Purcell 1981). Additional
658 details on the optimization are available in the Supplementary Materials.

659 To test how many times extreme nematocyst morphologies evolved, we reconstructed
660 the ancestral states of $\log(\text{length}/\text{width})$ of the different cnidoband nematocyst types, and
661 identified the branches with the greatest shifts. In addition to characterizing the shifts in the
662 state values of haploneme and heteroneme elongation, we identified and located regime shifts
663 for the rate of evolution using a Bayesian Analysis of Macroevolutionary Mixtures (BAMM)
664 (Rabosky et al. 2014) (SM32-35).

665 **Supplementary Materials**

666 Data available from the Dryad Digital Repository: <http://dx.doi.org/10.5061/dryad.NNNN>
667 Supplementary Materials are available in https://github.com/dunnlab/tentilla_morph/
668 Supplement_forShort.pdf

669 **Funding**

670 This work was supported by the Society of Systematic Biologists (Graduate Student Award
671 to A.D.S.); the Yale Institute of Biospheric Studies (Doctoral Pilot Grant to A.D.S.); and
672 the National Science Foundation (Waterman Award to C.W.D., and NSF-OCE 1829835 to
673 C.W.D., S.H.D.H., and C. Anela Choy). A.D.S. was supported by a Fulbright Spain Graduate
674 Studies Scholarship.

675 **Acknowledgements**

676 We wish to thank the crew and scientists of the R/V Western Flyer, who participated in
677 the collection of many of the specimens used in this study. We also want to thank Lynne

678 Christianson and Shannon Johnson from the Monterey Bay Aquarium Research Institute
679 for their assistance in the field as well as for sequencing some of the species included in this
680 phylogeny. In addition, we wish to thank Lourdes Rojas, Daniel Drew, and Eric Lazo-Wasem
681 for their assistance in imaging the fixed specimens and managing the collections. We thank
682 Dennis Pilarczyk for organizing the prey selectivity data, Michael Landis for helping design
683 the Bayesian analyses, and Joaquin Nunez for reviewing this manuscript. Furthermore, we
684 thank Elizabeth D. Hetherington and C. Anela Choy for collating the data on siphonophore
685 feeding and for reviewing the manuscript. Finally, we thank Philip Pugh, who confirmed
686 many of our specimen identifications and taught us valuable knowledge about siphonophores.

687 References

- 688 Andersen O.G.N. 1981. Redescription of *marrus orthocanna* (kramp, 1942)(Cnidaria,
689 siphonophora). Zoological Museum, University of Copenhagen.
- 690 Bardi J., Marques A.C. 2007. Taxonomic redescription of the portuguese man-of-war,
691 *physalia physalis* (cnidaria, hydrozoa, siphonophorae, cystonectae) from brazil. Iheringia.
692 Série Zoologia. 97:425–433.
- 693 Beaulieu J., O'Meara B. 2012. OUwie: Analysis of evolutionary rates in an ou framework.
694 R package version 1.17..
- 695 Biggs D.C. 1977. Field studies of fishing, feeding, and digestion in siphonophores. Marine
696 & Freshwater Behaviour & Phy. 4:261–274.
- 697 Blomberg S.P., Garland T., Ives A.R. 2003. Testing for phylogenetic signal in comparative
698 data: Behavioral traits are more labile. Evolution. 57:717–745.
- 699 Butler M.A., King A.A. 2004. Phylogenetic comparative analysis: A modeling approach
700 for adaptive evolution. The American Naturalist. 164:683–695.
- 701 Caetano D.S., Harmon L.J. 2018. Estimating correlated rates of trait evolution with
702 uncertainty. Systematic biology. 68:412–429.
- 703 Carré D. 1972. Study on development of cnidocysts in gastrozooids of *muggiaeae kochi*

- 704 (will, 1844) (siphonophora, calycophora). Comptes Rendus Hebdomadaires des Seances de
705 l'Academie des Sciences Serie D. 275:1263.
- 706 Carré D., Carré C. 1980. On triggering and control of cnidocyst discharge. Marine &
707 Freshwater Behaviour & Phy. 7:109–117.
- 708 Choy C.A., Haddock S.H., Robison B.H. 2017. Deep pelagic food web structure as revealed
709 by in situ feeding observations. Proceedings of the Royal Society B: Biological Sciences.
710 284:20172116.
- 711 Claverie T., Patek S. 2013. Modularity and rates of evolutionary change in a power-
712 amplified prey capture system. Evolution. 67:3191–3207.
- 713 Collar D.C., Near T.J., Wainwright P.C. 2005. Comparative analysis of morphological
714 diversity: Does disparity accumulate at the same rate in two lineages of centrarchid fishes?
715 Evolution. 59:1783–1794.
- 716 Collins T.J. 2007. ImageJ for microscopy. Biotechniques. 43:S25–S30.
- 717 Costello J.H., Colin S.P., Gemmell B.J., Dabiri J.O., Sutherland K.R. 2015. Multi-jet
718 propulsion organized by clonal development in a colonial siphonophore. Nature communica-
719 tions. 6:8158.
- 720 Cressler C.E., Butler M.A., King A.A. 2015. Detecting adaptive evolution in phylogenetic
721 comparative analysis using the ornstein–uhlenbeck model. Systematic biology. 64:953–968.
- 722 Cunningham C.W., Buss L.W. 1993. Molecular evidence for multiple episodes of paedo-
723 morphosis in the family hydractiniidae. Biochemical Systematics and Ecology. 21:57–69.
- 724 David C.N., Özbek S., Adamczyk P., Meier S., Pauly B., Chapman J., Hwang J.S.,
725 Gojobori T., Holstein T.W. 2008. Evolution of complex structures: Minicollagens shape the
726 cnidarian nematocyst. Trends in genetics. 24:431–438.
- 727 Dunn C.W., Pugh P.R., Haddock S.H. 2005. Molecular phylogenetics of the siphonophora
728 (cnidaria), with implications for the evolution of functional specialization. Systematic biology.
729 54:916–935.
- 730 Futuyma D.J., Moreno G. 1988. The evolution of ecological specialization. Annual review

- 731 of Ecology and Systematics. 19:207–233.
- 732 Goswami A. 2006. Morphological integration in the carnivoran skull. Evolution. 60:169–
733 183.
- 734 Grafen A. 1989. The phylogenetic regression. Philosophical Transactions of the Royal
735 Society of London. B, Biological Sciences. 326:119–157.
- 736 Haddock S.H., Dunn C.W. 2015. Fluorescent proteins function as a prey attractant:
737 Experimental evidence from the hydromedusa *olindias formosus* and other marine organisms.
738 Biology open. 4:1094–1104.
- 739 Haddock S.H., Dunn C.W., Pugh P.R., Schnitzler C.E. 2005. Bioluminescent and red-
740 fluorescent lures in a deep-sea siphonophore. Science. 309:263–263.
- 741 Haddock S.H., Heine J.N. 2005. Scientific blue-water diving. California Sea Grant College
742 Program.
- 743 Hallgrímsdóttir B., Jamniczky H.A., Young N.M., Rolian C., SCHMIDT-OTT U., Marcucio
744 R.S. 2012. The generation of variation and the developmental basis for evolutionary novelty.
745 Journal of Experimental Zoology Part B: Molecular and Developmental Evolution. 318:501–
746 517.
- 747 Hardin G. 1960. The competitive exclusion principle. science. 131:1292–1297.
- 748 Hardy N.B., Otto S.P. 2014. Specialization and generalization in the diversification of
749 phytophagous insects: Tests of the musical chairs and oscillation hypotheses. Proceedings of
750 the Royal Society B: Biological Sciences. 281:20132960.
- 751 Harmon L.J., Losos J.B., Jonathan Davies T., Gillespie R.G., Gittleman J.L., Bryan
752 Jennings W., Kozak K.H., McPeek M.A., Moreno-Roark F., Near T.J., others. 2010. Early
753 bursts of body size and shape evolution are rare in comparative data. Evolution: International
754 Journal of Organic Evolution. 64:2385–2396.
- 755 Harmon L.J., Weir J.T., Brock C.D., Glor R.E., Challenger W. 2007. GEIGER: Investi-
756 gating evolutionary radiations. Bioinformatics. 24:129–131.
- 757 Hessinger D.A. 1988. Nematocyst venoms and toxins. The biology of nematocysts.

- 758 Elsevier. p. 333–368.
- 759 Hissmann K. 2005. In situ observations on benthic siphonophores (physonectae: Rhodali-
760 idae) and descriptions of three new species from indonesia and south africa. Systematics and
761 Biodiversity. 2:223–249.
- 762 Hoberg E.P., Brooks D.R. 2008. A macroevolutionary mosaic: Episodic host-switching,
763 geographical colonization and diversification in complex host–parasite systems. Journal of
764 Biogeography. 35:1533–1550.
- 765 Höhna S., Landis M.J., Heath T.A., Boussau B., Lartillot N., Moore B.R., Huelsenbeck
766 J.P., Ronquist F. 2016. RevBayes: Bayesian phylogenetic inference using graphical models
767 and an interactive model-specification language. Systematic Biology. 65:726–736.
- 768 Hutchinson G.E. 1961. The paradox of the plankton. The American Naturalist. 95:137–
769 145.
- 770 Jacobs J. 1974. Quantitative measurement of food selection. Oecologia. 14:413–417.
- 771 Johnson K.P., Malenke J.R., Clayton D.H. 2009. Competition promotes the evolution of
772 host generalists in obligate parasites. Proceedings of the Royal Society B: Biological Sciences.
773 276:3921–3926.
- 774 Jombart T., Devillard S., Balloux F. 2010. Discriminant analysis of principal components:
775 A new method for the analysis of genetically structured populations. BMC genetics. 11:94.
- 776 Kalyaanamoorthy S., Minh B.Q., Wong T.K., Haeseler A. von, Jermiin L.S. 2017. Mod-
777 elFinder: Fast model selection for accurate phylogenetic estimates. Nature methods. 14:587.
- 778 Katoh K., Misawa K., Kuma K.-i., Miyata T. 2002. MAFFT: A novel method for
779 rapid multiple sequence alignment based on fast fourier transform. Nucleic acids research.
780 30:3059–3066.
- 781 Kayal E., Bentlage B., Cartwright P., Yanagihara A.A., Lindsay D.J., Hopcroft R.R.,
782 Collins A.G. 2015. Phylogenetic analysis of higher-level relationships within hydroidolina
783 (cnidaria: Hydrozoa) using mitochondrial genome data and insight into their mitochondrial
784 transcription. PeerJ. 3:e1403.

- 785 Longhurst A.R. 1985. The structure and evolution of plankton communities. *Progress in*
786 *Oceanography*. 15:1–35.
- 787 Mackie G.O., Pugh P.R., Purcell J.E. 1987. Siphonophore Biology. *Advances in Marine*
788 *Biology*. 24:97–262.
- 789 Mapstone G.M. 2014. Global diversity and review of siphonophorae (cnidaria: Hydrozoa).
790 *PLoS One*. 9:e87737.
- 791 Martins E.P. 1996. Phylogenies, spatial autoregression, and the comparative method: A
792 computer simulation test. *Evolution*. 50:1750–1765.
- 793 Monteiro L.R., Nogueira M.R. 2010. Adaptive radiations, ecological specialization, and
794 the evolutionary integration of complex morphological structures. *Evolution: International*
795 *Journal of Organic Evolution*. 64:724–744.
- 796 Munro C., Siebert S., Zapata F., Howison M., Serrano A.D., Church S.H., Goetz F.E.,
797 Pugh P.R., Haddock S.H., Dunn C.W. 2018. Improved phylogenetic resolution within
798 siphonophora (cnidaria) with implications for trait evolution. *Molecular Phylogenetics and*
799 *Evolution*.
- 800 Nguyen L.-T., Schmidt H.A., Haeseler A. von, Minh B.Q. 2014. IQ-tree: A fast and
801 effective stochastic algorithm for estimating maximum-likelihood phylogenies. *Molecular*
802 *biology and evolution*. 32:268–274.
- 803 Nosil P. 2002. Transition rates between specialization and generalization in phytophagous
804 insects. *Evolution*. 56:1701–1706.
- 805 Nosil P., Mooers A. 2005. Testing hypotheses about ecological specialization using
806 phylogenetic trees. *Evolution*. 59:2256–2263.
- 807 O'Brien T.D. 2007. COPEPOD, a global plankton database: A review of the 2007
808 database contents and new quality control methodology..
- 809 Pagel M. 1994. Detecting correlated evolution on phylogenies: A general method for the
810 comparative analysis of discrete characters. *Proceedings of the Royal Society of London*.
811 *Series B: Biological Sciences*. 255:37–45.

- 812 Paradis E., Blomberg S., Bolker B., Brown J., Claude J., Cuong H.S., Desper R. 2019.
- 813 Package “ape”. Analyses of phylogenetics and evolution, version.:2–4.
- 814 Pennell M.W., FitzJohn R.G., Cornwell W.K., Harmon L.J. 2015. Model adequacy and
- 815 the macroevolution of angiosperm functional traits. *The American Naturalist*. 186:E33–E50.
- 816 Pigliucci M. 2003. Phenotypic integration: Studying the ecology and evolution of complex
- 817 phenotypes. *Ecology Letters*. 6:265–272.
- 818 Pugh P. 2001. A review of the genus *erenna bedot*, 1904 (siphonophora, physonectae).
- 819 BULLETIN-NATURAL HISTORY MUSEUM ZOOLOGY SERIES. 67:169–182.
- 820 Pugh P., Youngbluth M. 1988. Two new species of prayine siphonophore (calycophorae,
821 prayidae) collected by the submersibles johnson-sea-link i and ii. *Journal of Plankton Research*.
822 10:637–657.
- 823 Purcell J. 1981. Dietary composition and diel feeding patterns of epipelagic siphonophores.
- 824 *Marine Biology*. 65:83–90.
- 825 Purcell J.E. 1980. Influence of siphonophore behavior upon their natural diets: Evidence
826 for aggressive mimicry. *Science*. 209:1045–1047.
- 827 Purcell J.E. 1984. The functions of nematocysts in prey capture by epipelagic
828 siphonophores (coelenterata, hydrozoa). *The Biological Bulletin*. 166:310–327.
- 829 Purcell J., Mills C. 1988. The correlation of nematocyst types to diets in pelagic hydrozoa.
830 In “the biology of nematocysts”.(Eds da hessinger and hm lenhoff.) pp. 463–485..
- 831 Rabosky D.L., Grundler M., Anderson C., Title P., Shi J.J., Brown J.W., Huang H.,
832 Larson J.G. 2014. BAMM tools: An r package for the analysis of evolutionary dynamics on
833 phylogenetic trees. *Methods in Ecology and Evolution*. 5:701–707.
- 834 Revell L.J. 2012. Phytools: An r package for phylogenetic comparative biology (and other
835 things). *Methods in Ecology and Evolution*. 3:217–223.
- 836 Revell L.J., Collar D.C. 2009. Phylogenetic analysis of the evolutionary correlation using
837 likelihood. *Evolution: International Journal of Organic Evolution*. 63:1090–1100.
- 838 Robison B.H. 2004. Deep pelagic biology. *Journal of experimental marine biology and*

- 839 ecology. 300:253–272.
- 840 Schindelin J., Arganda-Carreras I., Frise E., Kaynig V., Longair M., Pietzsch T., Preibisch
841 S., Rueden C., Saalfeld S., Schmid B., others. 2012. Fiji: An open-source platform for
842 biological-image analysis. *Nature methods*. 9:676.
- 843 Schluter D. 2000. Ecological character displacement in adaptive radiation. *the american
844 naturalist*. 156:S4–S16.
- 845 Schmitz O. 2017. Predator and prey functional traits: Understanding the adaptive
846 machinery driving predator–prey interactions. *F1000Research*. 6.
- 847 Shapiro S.S., Wilk M.B. 1965. An analysis of variance test for normality (complete
848 samples). *Biometrika*. 52:591–611.
- 849 Siebert S., Pugh P.R., Haddock S.H., Dunn C.W. 2013. Re-evaluation of characters in
850 apolemiidae (siphonophora), with description of two new species from monterey bay, california.
851 *Zootaxa*. 3702:201–232.
- 852 Simpson G.G. 1944. *Tempo and mode in evolution*. Columbia University Press.
- 853 Skaer R. 1988. The formation of cnidocyte patterns in siphonophores. Academic Press
854 New York.
- 855 Skaer R. 1991. Remodelling during the development of nematocysts in a siphonophore.
856 *Hydrobiologia*. 216:685–689.
- 857 Stireman-III J.O. 2005. The evolution of generalization? Parasitoid flies and the perils of
858 inferring host range evolution from phylogenies. *Journal of evolutionary biology*. 18:325–336.
- 859 Sugiura N. 1978. Further analysts of the data by akaike's information criterion and the
860 finite corrections: Further analysts of the data by akaike's. *Communications in Statistics-
861 Theory and Methods*. 7:13–26.
- 862 Team R.C. 2017. *R: A language and environment for statistical computing*. Vienna,
863 austria: R foundation for statistical computing; 2017..
- 864 Thomason J. 1988. The allometry of nematocysts. *The biology of nematocysts*. Elsevier.
865 p. 575–588.

- 866 Totton A.K., Bargmann H.E. 1965. A synopsis of the siphonophora. British Museum
867 (Natural History).
- 868 Uhlenbeck G.E., Ornstein L.S. 1930. On the theory of the brownian motion. Physical
869 review. 36:823.
- 870 Wagner G.P., Schwenk K. 2000. Evolutionarily stable configurations: Functional in-
871 tegration and the evolution of phenotypic stability. Evolutionary biology. Springer. p.
872 155–217.
- 873 Young N.M., Hallgrímsson B. 2005. Serial homology and the evolution of mammalian
874 limb covariation structure. Evolution. 59:2691–2704.